

## THERMAL DECOMPOSITION OF HYDROCERUSSITE ( $2 \text{PbCO}_3 \cdot \text{Pb}(\text{OH})_2$ ) IN CARBON DIOXIDE ATMOSPHERE (0–50 atm)

JUNJI YAMAGUCHI, YUTAKA SAWADA \*, OSAMU SAKURAI, KEIZO UEMATSU, NOBUYASU MIZUTANI and MASANORI KATO \*\*

*Department of Inorganic Materials, Faculty of Engineering, Tokyo Institute of Technology, O-okayama, Meguro-ku, Tokyo 152 (Japan)*

(Received 27 August 1979)

### ABSTRACT

The thermal decomposition of hydrocerussite was studied with TG, high-pressure DTA and powder X-ray diffraction techniques in the  $p_{\text{CO}_2}$  range 0–50 atm. The decomposition process was strongly affected by  $p_{\text{CO}_2}$ .  $\text{PbCO}_3$ , as a new intermediate, was found at carbon dioxide pressures above 1 atm. The results were different from any of the previous studies. The temperatures of all the endothermic processes increased and the formation temperature of  $\text{PbCO}_3$  decreased with increasing  $p_{\text{CO}_2}$ . The results are discussed by referring to the equilibrium phase diagram of the system  $\text{PbO}-\text{CO}_2$ .

### INTRODUCTION

The thermal decomposition of hydrocerussite proceeds via dehydration and decarbonation to  $\text{PbO}$  and many oxycarbonate intermediates appear in this decomposition process. The number and the kind of intermediates involved in the process and their decomposition temperatures are clearly affected by the carbon dioxide pressure,  $p_{\text{CO}_2}$ .

This paper presents the thermal decomposition of hydrocerussite studied with TG, high-pressure DTA and powder X-ray diffraction techniques in a wide pressure range of carbon dioxide. No worker has studied the effect of carbon dioxide pressure on the thermal decomposition of hydrocerussite systematically.

Pannetier et al. [1] investigated the thermal decomposition of hydrocerussite in a carbon dioxide atmosphere with TG, DTA and powder X-ray diffraction techniques. Dehydration took place at  $170^\circ\text{C}$  and an oxycarbonate intermediate,  $2 \text{PbCO}_3 \cdot \text{PbO}$ , was formed. This intermediate decomposed to another intermediate,  $\text{PbCO}_3 \cdot 2 \text{PbO}$ , at  $300^\circ\text{C}$  with evolution of carbon dioxide. The final product,  $\text{PbO}$ , was formed at  $420^\circ\text{C}$ .

The TG and DTA studies of Sarig and Kahana [2] in an argon atmosphere showed that hydrocerussite decomposed at  $140^\circ\text{C}$  with evolution of water

---

\* Present address: Toyota Central Research and Development Laboratories, 2-12 Hisakata, Tenpaku-ku, Nagoya 468, Japan.

\*\* To whom correspondence should be addressed.

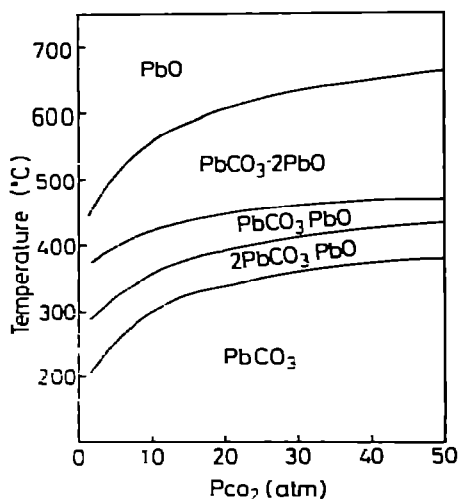


Fig. 1. Phase diagram of the system PbO—CO<sub>2</sub> [4]

vapor to  $2 \text{PbCO}_3 \cdot \text{PbO}$  which then decomposed to  $2 \text{PbCO}_3 \cdot 3 \text{PbO}$  at  $240^\circ\text{C}$  with evolution of carbon dioxide and finally to PbO at  $320^\circ\text{C}$ , again with evolution of carbon dioxide.

The results of Andreeva and Limar [3] with TG, DTA, IR and powder X-ray diffraction analysis were different from those of the above two studies. No description of the atmosphere was given in their study but it was probably carbon dioxide. They postulated the following process; hydrocerussite decomposed at  $240^\circ\text{C}$  to  $2 \text{PbCO}_3 \cdot \text{PbO}$  which successively decomposed at  $348\text{--}350^\circ\text{C}$  to  $\text{PbCO}_3 \cdot \text{PbO}$ , at  $390\text{--}400^\circ\text{C}$  to  $\text{PbCO}_3 \cdot 2 \text{PbO}$  and at  $450\text{--}470^\circ\text{C}$  to PbO.

In the present study, the thermal decomposition of hydrocerussite is studied in the  $p_{\text{CO}_2}$  range 0—50 atm. The decomposition process was strongly affected by  $p_{\text{CO}_2}$  and a new intermediate,  $\text{PbCO}_3$ , was found at  $p_{\text{CO}_2} > 1$  atm. The results differ from those of the previous studies. The decomposition processes are explained by referring to the equilibrium phase diagram at  $p_{\text{CO}_2} > 3$  atm. Figure 1 shows the equilibrium diagram of the system PbO—CO<sub>2</sub> [4]. No phase diagram is reported for the system PbO—CO<sub>2</sub>—H<sub>2</sub>O.

## EXPERIMENTAL

### Samples

Reagent grade basic lead carbonate (Kanto Chemical Co., Inc., Japan) was used as hydrocerussite. The PbO : CO<sub>2</sub> : H<sub>2</sub>O molar ratio (1.00 : 0.70 : 0.28), determined by the compositional analysis, was approximately equal to that of the pure hydrocerussite  $2 \text{PbCO}_3 \cdot \text{Pb(OH)}_2$  (1.00 : 0.66 : 0.33) and powder X-ray diffraction showed the pattern of hydrocerussite (JCPDS 13-131). The particles were block shaped and the SEM micrograph (Fig. 2) showed them to be larger than 1  $\mu\text{m}$ .

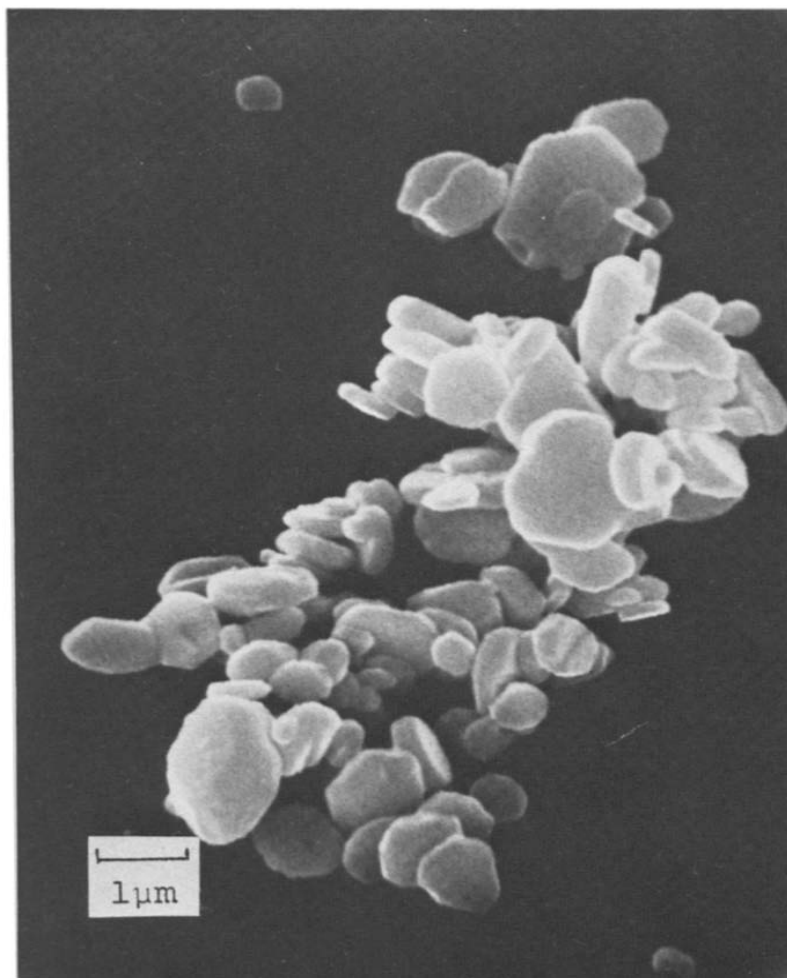


Fig. 2. SEM micrograph of hydrocerussite.

### *High-pressure differential thermal analysis*

The decomposition process was studied in detail using a high-pressure DTA apparatus which was newly designed and constructed by the authors [5]. The specimen was heated under various pressures of carbon dioxide ( $p_{\text{CO}_2} \leq 50$  atm) at a heating rate of  $\sim 10^\circ\text{C min}^{-1}$  up to  $700^\circ\text{C}$ . The atmosphere in the specimen chamber was changed to pure carbon dioxide by flushing the chamber with the gas three times before the experiment was carried out. Carbon dioxide was then passed through this chamber ( $100\text{ ml min}^{-1}$ ) to remove the gases evolved on thermal decomposition rapidly.

### *Differential thermal analysis and thermogravimetry*

The DTA–TG apparatus (Type M8076, Rigaku Denki Co., Japan) was used in air and a stream of carbon dioxide ( $p_{\text{CO}_2} = 1$  atm, flow rate  $60\text{ ml min}^{-1}$ ); the heating rate was  $\sim 10^\circ\text{C min}^{-1}$ .

### *X-Ray powder diffraction*

The structural changes in the specimen were examined by a X-ray diffractometer (APD-10, Philips Co.) with Cu target and monochromator. The specimens at  $p_{\text{CO}_2} \leq 3$  atm were prepared by quenching from various temperatures in air. At  $p_{\text{CO}_2} > 3$  atm, the specimens were cooled at  $\sim 20^\circ\text{C min}^{-1}$  from various temperatures in the high-pressure DTA with the high-pressure carbon dioxide released simultaneously. It was ascertained by high-pressure DTA that no reaction occurred during the cooling process.

### RESULTS

A total of over 100 runs were made in the  $p_{\text{CO}_2}$  range 0–50 atm. Figure 3 shows representative DTA diagrams for the thermal decomposition of hydrocerussite at various carbon dioxide pressures. The strong influence of  $p_{\text{CO}_2}$  on the thermal decomposition of hydrocerussite is clearly seen. The number of intermediates involved in the decomposition process (endothermic peaks) increased with increasing  $p_{\text{CO}_2}$ , and at a pressure above approximately 1 atm,  $\text{PbCO}_3$  was formed (endothermic peak at  $\sim 220^\circ\text{C}$ ). As described in detail below, with increasing  $p_{\text{CO}_2}$ , the decomposition temperature of each intermediate increased and the formation temperature of  $\text{PbCO}_3$  decreased. Decomposition of hydrocerussite could be divided into four groups at various

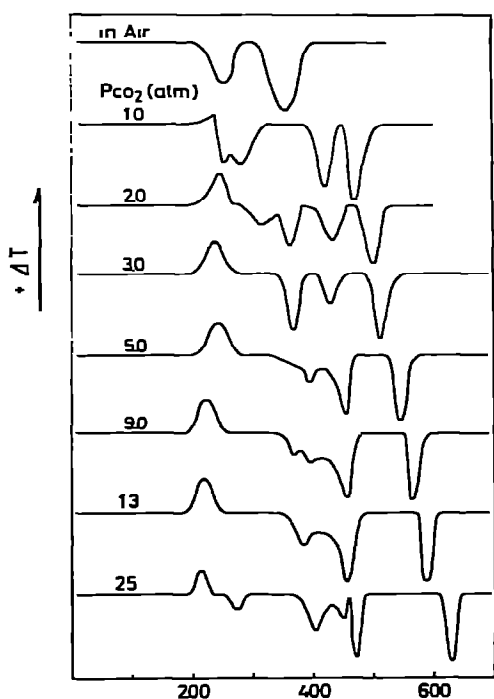


Fig. 3. DTA of hydrocerussite at the carbon dioxide pressures shown.

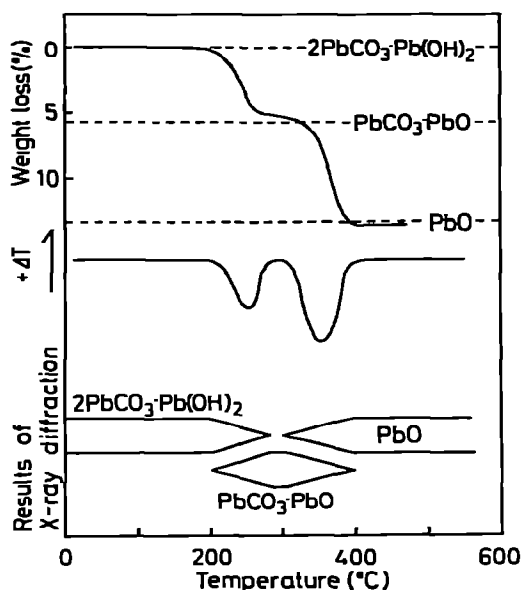


Fig. 4. DTA—TG and the results of X-ray diffraction analysis on the thermal decomposition of hydrocerussite in air. The dotted lines show the calculated weight loss for the formation of each compound. The width of the band in the X-ray diffraction analysis represents the approximate amount of phase present in the specimen.

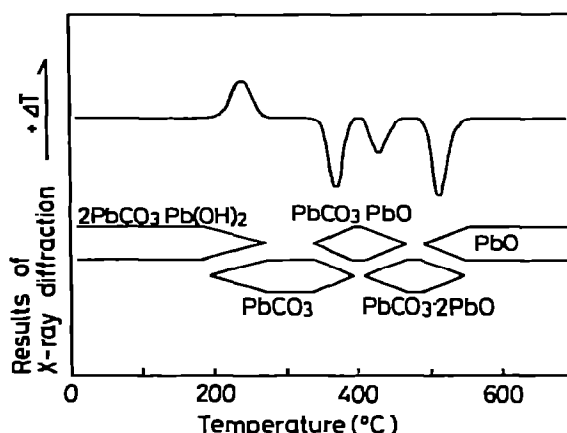


Fig. 5. DTA and the results of X-ray diffraction analysis on the thermal decomposition of hydrocerussite at  $p_{\text{CO}_2} = 3 \text{ atm}$ . The width of the band in the X-ray diffraction analysis represents the approximate amount of phase present in the specimen.

carbon dioxide pressures. Decomposition process belonging to the neighbouring group often occurred simultaneously at the transition region of the groups.

$p_{\text{CO}_2} \ll 1 \text{ atm (in air)}$

Figure 4 shows the results of TG and DTA, and the phases identified by X-ray diffraction analysis on the specimens quenched from various temperatures. Two endothermic peaks at  $\sim 250^\circ\text{C}$  and  $\sim 340^\circ\text{C}$  and weight losses at  $\sim 200\text{--}270^\circ\text{C}$  and  $\sim 330\text{--}400^\circ\text{C}$  were found in DTA and TG, respectively. The phases identified at various temperatures were  $2 \text{ PbCO}_3 \cdot \text{Pb(OH)}_2$  below  $\sim 280^\circ\text{C}$ ,  $\text{PbCO}_3 \cdot \text{PbO}$  at  $\sim 200\text{--}400^\circ\text{C}$ , and  $\text{PbO}$  above  $\sim 300^\circ\text{C}$ .

$\sim 1 \text{ atm} \leq p_{\text{CO}_2} < \sim 5 \text{ atm}$

Figure 5 shows the results of the DTA and X-ray diffraction analysis on specimens quenched from various temperatures at a carbon dioxide pressure of 3 atm. One exothermic peak at  $\sim 240^\circ\text{C}$  and three endothermic peaks at  $\sim 370$ ,  $\sim 430$  and  $\sim 570^\circ\text{C}$  can be seen. The phases identified at various temperatures were  $2 \text{ PbCO}_3 \cdot \text{Pb(OH)}_2$  below  $\sim 270^\circ\text{C}$ ,  $\text{PbCO}_3$  at  $\sim 200\text{--}390^\circ\text{C}$ ,  $\text{PbCO}_3 \cdot \text{PbO}$  at  $\sim 330\text{--}460^\circ\text{C}$ ,  $\text{PbCO}_3 \cdot 2 \text{ PbO}$  at  $\sim 410\text{--}550^\circ\text{C}$ , and  $\text{PbO}$

above  $\sim 500^\circ\text{C}$ . The exothermic peak obtained by DTA became stronger and moved towards lower temperatures with increasing  $p_{\text{CO}_2}$ . This exothermic peak was clearly due to the formation of cerussite,  $\text{PbCO}_3$ , from hydrocerussite and carbon dioxide in the atmosphere. With decreasing  $p_{\text{CO}_2}$ , the fraction of  $\text{PbCO}_3$  in the quenched specimen decreased. At  $p_{\text{CO}_2} = 1$  atm, the exothermic peak was very weak and was followed by strong endothermic peaks. The constitution of the specimen quenched immediately after the first endothermic peak was mostly  $\text{PbCO}_3 \cdot \text{PbO}$  with minor amounts of  $\text{PbCO}_3$  and  $\text{PbCO}_3 \cdot 2 \text{PbO}$ . The endothermic peak which followed immediately after the exothermic peak became weaker and moved towards higher temperatures with the increasing  $p_{\text{CO}_2}$ .

$\sim 5 \text{ atm} \leq p_{\text{CO}_2} < \sim 15 \text{ atm}$

Figure 6 shows the results of DTA and X-ray diffraction analysis on the specimens cooled from various temperatures at a carbon dioxide pressure of 9 atm. An exothermic peak at  $\sim 220^\circ\text{C}$  and four endothermic peaks at  $\sim 370$ ,  $\sim 400$ ,  $\sim 460$  and  $\sim 560^\circ\text{C}$  were found. The phases identified by X-ray diffraction analysis were  $2 \text{PbCO}_3 \cdot \text{Pb}(\text{OH})_2$  below  $\sim 260^\circ\text{C}$ ,  $\text{PbCO}_3$  at  $\sim 200$ – $450^\circ\text{C}$ ,  $2 \text{PbCO}_3 \cdot \text{PbO}$  at  $\sim 340$ – $460^\circ\text{C}$ ,  $\text{PbCO}_3 \cdot \text{PbO}$  at  $\sim 360$ – $480^\circ\text{C}$ ,  $\text{PbCO}_3 \cdot 2 \text{PbO}$  at  $\sim 410$ – $590^\circ\text{C}$ , and  $\text{PbO}$  above  $\sim 550^\circ\text{C}$ . With increasing  $p_{\text{CO}_2}$ , the peak temperatures of all the endothermic decomposition processes increased and that of the exothermic process decreased. In the temperature range  $\sim 350$ – $450^\circ\text{C}$ , three or four intermediates coexisted. At  $p_{\text{CO}_2} = 5$  and 13 atm in Fig. 3, the number of clear peaks in the DTA apparently decreased; however, the same four intermediates described above were found at various temperatures by X-ray diffraction analysis.

$\sim 15 \text{ atm} < p_{\text{CO}_2}$

Figure 7 shows the results of DTA and X-ray diffraction analysis on the specimens cooled from various temperatures at a carbon dioxide pressure of 25 atm. The intermediates appearing in this  $p_{\text{CO}_2}$  region were the same as those found at 5–15 atm. However, the decomposition process was more complicated. A new endothermic peak appeared at the temperature close to the exothermic peak. The endothermic peak was absent at  $p_{\text{CO}_2} < \sim 15$  atm. A significant amount of hydrocerussite starting material, as well as  $\text{PbCO}_3$  was found in the specimen cooled immediately after the exothermic peak. The specimen cooled immediately after the first endothermic peak contained only  $\text{PbCO}_3$  according to X-ray diffraction analysis. Apparently, the formation of  $\text{PbCO}_3$  from the starting material after the exothermic peak and the carbon dioxide in the atmosphere is endothermic under these conditions. The process that followed this endothermic peak at higher temperatures was essentially the same as that found at  $p_{\text{CO}_2} = \sim 5$ – $15$  atm. The phases identified by X-ray diffraction analysis on the cooled specimens were  $2 \text{PbCO}_3 \cdot \text{Pb}(\text{OH})_2$  below  $\sim 290^\circ\text{C}$ ,  $\text{PbCO}_3$  at  $\sim 190$ – $430^\circ\text{C}$ ,  $2 \text{PbCO}_3 \cdot \text{PbO}$  at  $\sim 370$ – $470^\circ\text{C}$ ,  $\text{PbCO}_3 \cdot \text{PbO}$  at  $\sim 430$ – $490^\circ\text{C}$ ,  $\text{PbCO}_3 \cdot 2 \text{PbO}$  at  $\sim 470$ – $650^\circ\text{C}$ , and  $\text{PbO}$  above  $\sim 620^\circ\text{C}$ .

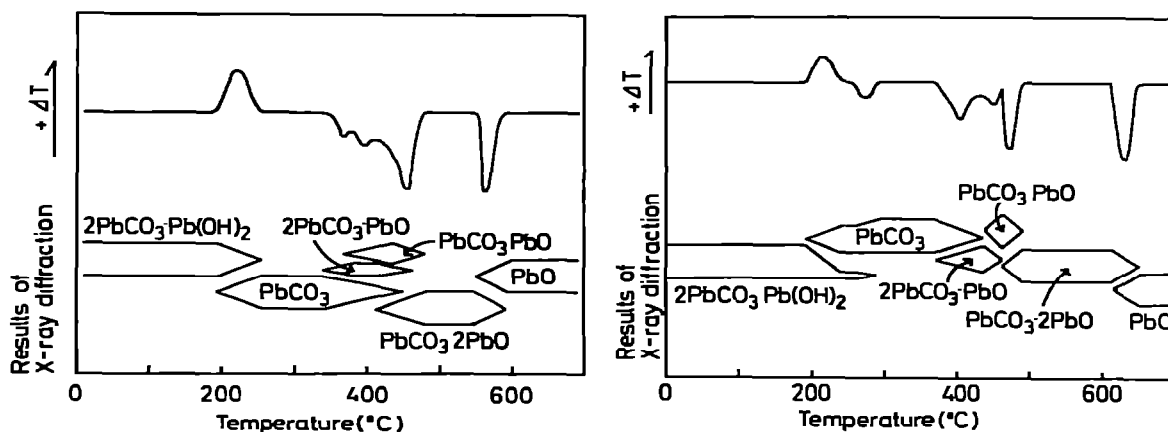


Fig. 6. DTA and the results of X-ray diffraction analysis on the thermal decomposition of hydrocerussite at  $p_{\text{CO}_2} = 9$  atm. The width of band in the X-ray diffraction analysis represents the approximate amount of phase present in the specimen.

Fig. 7. DTA and the results of X-ray diffraction analysis on the thermal decomposition of hydrocerussite at  $p_{\text{CO}_2} = 25$  atm. The width of band in the X-ray diffraction analysis represents the approximate amount of phase in the specimen.

The peak DTA temperatures at various  $\text{CO}_2$  pressures are shown in Fig. 8. With increasing  $p_{\text{CO}_2}$ , the temperature of all the endothermic peaks increased except for the curious endothermic peak at the  $p_{\text{CO}_2} > \sim 15$  atm, but that of the exothermic peak decreased. The peak DTA temperature after dehydration lay near the equilibrium phase boundaries of the system  $\text{PbO}-\text{CO}_2$  (Fig. 1). The peak temperatures were always higher than the temperatures of the equilibrium phase boundaries.

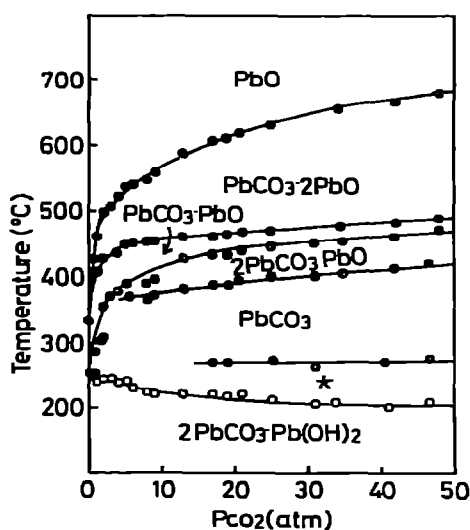
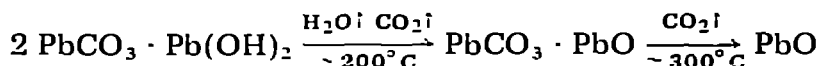


Fig. 8. Effect of  $p_{\text{CO}_2}$  on the peak temperature of various decomposition processes. The approximately horizontal line starting at  $p_{\text{CO}_2} = \sim 15$  atm shows the first endothermic peak temperature as shown on the DTA curve at  $p_{\text{CO}_2} = 25$  atm in Fig. 3, for example \* The details of this phase will be described in the Discussion.

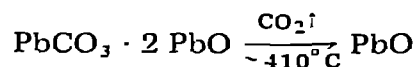
## DISCUSSION

Typical thermal decomposition processes of hydrocerussite at various  $\text{CO}_2$  pressures are summarized below.

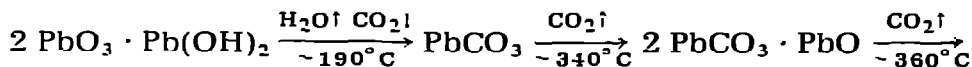
*Process 1 (in air)*



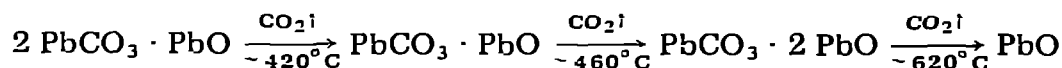
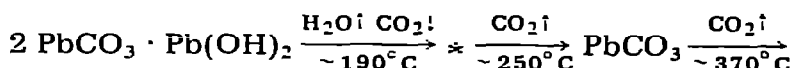
*Process 2 ( $p_{\text{CO}_2} = 3 \text{ atm}$ )*



*Process 3 ( $p_{\text{CO}_2} = 9 \text{ atm}$ )*



*Process 4 ( $p_{\text{CO}_2} = 25 \text{ atm}$ )*



This study is the first to show the formation of  $\text{PbCO}_3$ .

In air, only one intermediate,  $\text{PbCO}_3 \cdot \text{PbO}$ , was involved in the thermal decomposition process. Hydrocerussite decomposed to  $\text{PbCO}_3 \cdot \text{PbO}$  with the simultaneous evolution of carbon dioxide and water vapor.  $\text{PbO}$  was formed at  $\sim 300^\circ\text{C}$ . This result is different from that of Sarig and Kahana [2] who proposed two intermediates,  $2 \text{PbCO}_3 \cdot \text{PbO}$  and  $2 \text{PbCO}_3 \cdot 3 \text{PbO}$ , in their thermal decomposition study of hydrocerussite in an argon atmosphere. Detailed discussion is not attempted here since these authors arrived at their conclusion from only the TG study; no X-ray diffraction analysis was made.

The decomposition process 1 is unfavorable at  $\text{CO}_2$  pressures above 1 atm. An intermediate  $\text{PbCO}_3$  appeared at  $p_{\text{CO}_2} = 1 \text{ atm}$ . The fraction of hydrocerussite converted to  $\text{PbCO}_3$  increased with the increasing  $p_{\text{CO}_2}$  which suggests that  $\text{PbCO}_3$  is more stable than  $\text{PbCO}_3 \cdot \text{PbO}$  in this  $p_{\text{CO}_2}$  range at this temperature and that the formation of  $\text{PbCO}_3$  is governed by the supply of

\* The details of this phase are described below.

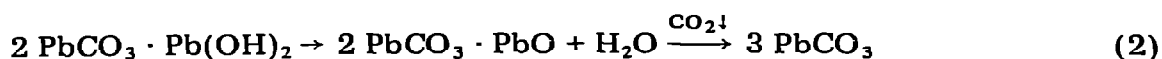
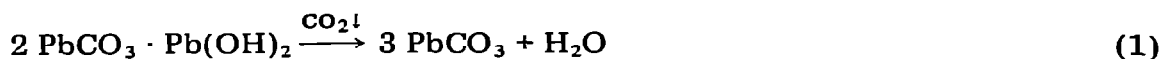


carbon dioxide from the gas phase. At low  $p_{\text{CO}_2}$ , the supply of carbon dioxide is insufficient to convert the hydrocerussite completely to  $\text{PbCO}_3$  and a large proportion of the hydrocerussite was decomposed to  $\text{PbCO}_3 \cdot \text{PbO}$  and  $2 \text{PbCO}_3 \cdot \text{PbO}$ . This decomposition process would probably disappear if the heating rate in the experiment was much lower. It is interesting to note that the decomposition temperature of this process also increased with increasing  $p_{\text{CO}_2}$ .

$\text{PbCO}_3$ ,  $\text{PbCO}_3 \cdot \text{PbO}$  and small amount of  $2 \text{PbCO}_3 \cdot \text{PbO}$  apparently coexisted at  $\sim 240\text{--}320^\circ\text{C}$  at  $p_{\text{CO}_2} = 1 \text{ atm}$ . All of them decomposed to  $\text{PbCO}_3 \cdot 2 \text{PbO}$  at  $\sim 390^\circ\text{C}$ ; apparently, the stability of these intermediates relative to  $\text{PbCO}_3 \cdot 2 \text{PbO}$  is rather similar. The result presented in Fig. 3 is different from that of Pannetier et al. [1] who studied the thermal decomposition of hydrocerussite under similar conditions. They proposed two intermediates,  $2 \text{PbCO}_3 \cdot \text{PbO}$  and  $\text{PbCO}_3 \cdot 2 \text{PbO}$ , at  $\sim 170\text{--}380^\circ\text{C}$  and  $\sim 300\text{--}470^\circ\text{C}$ , respectively. The presence of  $2 \text{PbCO}_3 \cdot \text{PbO}$  under these conditions was probably erroneous. In our study, only a small fraction of hydrocerussite was converted to  $2 \text{PbCO}_3 \cdot \text{PbO}$ . A considerable amount of  $2 \text{PbCO}_3 \cdot \text{PbO}$  was formed only when the  $p_{\text{CO}_2}$  exceeded 5 atm and its X-ray diffraction pattern agreed with that reported by Grisafe and White [4]. The X-ray diffraction pattern of the intermediate identified as  $2 \text{PbCO}_3 \cdot \text{PbO}$  by Pannetier et al. differs from those determined by ourselves and by Grisafe and White. We made a reassessment of their X-ray diffraction pattern and found that all the diffraction peaks could be identified successfully provided that the specimen consisted mostly of a mixture of  $\text{PbCO}_3$  and  $\text{PbCO}_3 \cdot \text{PbO}$ , which is in approximate agreement with our result.

The thermal decomposition of hydrocerussite at  $\text{CO}_2$  pressures above 3 atm could be explained by reference to the phase diagram of the system  $\text{PbO}\text{--}\text{CO}_2$  extrapolated to low  $p_{\text{CO}_2}$ . After the hydrocerussite was completely converted to  $\text{PbCO}_3$  at  $\sim 200\text{--}280^\circ\text{C}$ , the decomposition behavior which followed was essentially the same as that of  $\text{PbCO}_3$ . The peak temperatures for a given decomposition process lay very close to the corresponding equilibrium phase boundary. The slight difference of temperatures in the DTA peak and the equilibrium boundary is due to the low reaction rate for the process.

The formation mechanism of  $\text{PbCO}_3$  from hydrocerussite and carbon dioxide in the gas phase is interesting. There are at least two possibilities, (1)  $\text{H}_2\text{O}$  in the hydrocerussite is exchanged directly by the carbon dioxide in the gas phase, and (2) an oxycarbonate intermediate was formed and was immediately converted to  $\text{PbCO}_3$  by the reaction between this intermediate and the carbon dioxide in the gas phase.



In eqn. (2), the oxycarbonate intermediate was tentatively assumed to be  $2 \text{PbCO}_3 \cdot \text{PbO}$ . The direct exchange presented in eqn. (1) is more likely. In the mechanism shown in eqn. (1), the peak temperature of the exothermic

reaction decreased with increasing  $p_{\text{CO}_2}$  which is in agreement with experiment. In the mechanism shown in eqn. (2), the peak temperature for the intermediate oxycarbonate formation would be independent of  $p_{\text{CO}_2}$  and an endothermic peak would be expected in the DTA diagram immediately before the exothermic peak, especially at low  $p_{\text{CO}_2}$ , both of which are in disagreement with the experimental results.

Many intermediates were present in the temperature range  $\sim 340\text{--}480^\circ\text{C}$  at  $p_{\text{CO}_2} = 9$  atm. The coexistence of intermediates could be explained by the low rate of thermal decomposition. Referring to the phase diagram (Fig. 1), these intermediates,  $\text{PbCO}_3$ ,  $2 \text{PbCO}_3 \cdot \text{PbO}$ ,  $\text{PbCO}_3 \cdot \text{PbO}$  and  $\text{PbCO}_3 \cdot 2 \text{PbO}$  could exist at  $p_{\text{CO}_2} = 9$  atm in the temperature range  $\sim 190\text{--}450^\circ\text{C}$ ,  $\sim 340\text{--}460^\circ\text{C}$ ,  $\sim 360\text{--}480^\circ\text{C}$  and  $\sim 410\text{--}590^\circ\text{C}$ , respectively. The intermediate  $\text{PbCO}_3$  probably began to decompose to  $2 \text{PbCO}_3 \cdot \text{PbO}$  at  $\sim 340^\circ\text{C}$  but with a very low rate. Before all the  $\text{PbCO}_3$  decomposed to  $2 \text{PbCO}_3 \cdot \text{PbO}$ , the temperature increased and the next oxycarbonate,  $\text{PbCO}_3 \cdot \text{PbO}$ , became more stable than  $2 \text{PbCO}_3 \cdot \text{PbO}$ . The considerable fraction of  $\text{PbCO}_3$  still left in the specimen started to decompose to  $\text{PbCO}_3 \cdot \text{PbO}$  and/or  $2 \text{PbCO}_3 \cdot \text{PbO}$  and  $\text{PbCO}_3 \cdot \text{PbO}$ . At this stage, it cannot be determined whether  $\text{PbCO}_3$  decomposes to  $\text{PbCO}_3 \cdot \text{PbO}$  directly or through the intermediate  $2 \text{PbCO}_3 \cdot \text{PbO}$  (or to  $\text{PbCO}_3 \cdot \text{PbO}$  and  $2 \text{PbCO}_3 \cdot \text{PbO}$  simultaneously). As the temperature was increased further, at  $\sim 410\text{--}590^\circ\text{C}$ ,  $\text{PbCO}_3 \cdot 2 \text{PbO}$  became the most stable of the various intermediates. The other intermediates then began to decompose to  $\text{PbCO}_3 \cdot 2 \text{PbO}$ . Above  $\sim 480^\circ\text{C}$ , this intermediate finally decomposed to  $\text{PbO}$ . The presence of many intermediates at the transition region of groups can be explained in the same way.

The decomposition behavior at carbon dioxide pressures above  $\sim 15$  atm (Fig. 7) was puzzling. The phase diagram did not predict the change of decomposition behavior. The low reaction rate is not responsible for this change. The reaction rate generally increased with increasing temperature. The increased reaction temperature at high  $p_{\text{CO}_2}$  for a given decomposition process should increase the reaction rate and cause the decomposition to occur near the equilibrium condition. The result was tentatively explained by assuming an intermediate which contains more  $\text{CO}_2$  (or  $\text{CO}_3$ ) than  $\text{PbCO}_3$  and forms a dense gas-tight layer on the surface of specimen particles. The exchange reaction of  $\text{CO}_2$  and  $\text{H}_2\text{O}$  in the hydrocerussite was inhibited by the low transport rate of gas through this layer. The decomposition of this intermediate at higher temperature results in an endothermic DTA peak and the formation of  $\text{PbCO}_3$ . This explanation is far from complete. Further study is clearly needed to give a more satisfactory explanation.

## REFERENCES

- 1 G. Pannetier, S. Fenostein and L. Davignon, *Bull. Soc. Chim. Fr.*, (1965) 109.
- 2 S. Sarig and F. Kahana, *Thermochim. Acta*, 14 (1976) 263.
- 3 V.N. Andreeva and T.F. Limar, *Russ. J. Inorg. Chem.*, 15 (1970) 1077.
- 4 D.A. Grisafe and W.B. White, *Am. Mineral.*, 49 (1964) 1184.
- 5 Y. Sawada, J. Yamaguchi, O. Sakurai, K. Uematsu, N. Mizutani and M. Kato, *Thermochim. Acta*, 32 (1979) 277.